


SCIENTIFIC REPORTS



OPEN

Superior electric storage on an amorphous perfluorinated polymer surface

Mikio Fukuhara^{1,2}, Tomoyuki Kuroda¹, Fumihiko Hasegawa¹ & Takashi Sueyoshi³

Received: 22 October 2015
Accepted: 05 February 2016
Published: 23 February 2016

Amorphous perfluoroalkenyl vinyl ether polymer devices can store a remarkably powerful electric charge because their surface contains nanometre-sized cavities that are sensitive to the so-called quantum-size effect. With a work function of approximately 10 eV, the devices show a near-vertical line in the Nyquist diagram and a horizontal line near the -90° phase angle in the Bode diagram. Moreover, they have an integrated effect on the surface area for constant current discharging. This effect can be explained by the distributed constant electric circuit with a parallel assembly of nanometre-sized capacitors on a highly insulating polymer. The device can illuminate a red LED light for 3 ms after charging it with 1 mA at 10V. Further gains might be attained by integrating polymer sheets with a micro-electro mechanical system.

Storage systems for electrical energy have been investigated extensively over the past three decades^{1–5}. Efficient, high-energy-density electrical energy storage systems play an important role as a power source for devices such as batteries, fuel cells, and electric double-layer capacitors (EDLCs)^{3–5}, and they provide an effective power supply from the grid. Compared to batteries, EDLCs are more powerful and possess a longer cycle-life. EDLCs have some practical disadvantages, however, such as narrow operating temperatures between 253–323 K, a voltage limitation of 3 V for nonaquatic electric solutions, and poor AC electric storage.

To develop solid supercapacitors without liquid solvents, we studied the capacitance of nanocrystalline de-alloyed Si–Al alloy ribbons^{6,7} and de-alloyed and anodic oxidized Ti–Ni–Si alloy ribbons^{8,9}. These materials store AC electricity from 193–453 K with a voltage variation between 10–150 V and a DC capacitance of ~ 4.8 F (~ 52.8 kF/cm³). A common requirement for electric storage is a surface with nanometre-sized cavities and high electrical resistance. We assumed a surface structure consisting of a distributed constant-equivalent circuit of resistance and capacitance, and one that is analogous to the active carbons in EDLCs.

We report here about the superior electric storage on a polymer with high electrical resistance. We selected amorphous perfluoroalkenyl vinyl ether polymer (APVEP) film, CYTOP™ (EGG, Asahi Glass) with nanometre clusters containing the organic siloxanes. The fluorine atom is well known as the most electronegative element in the contact electrification series¹⁰. Our results show that the insulating amorphous perfluorinated-polymer (APP) film with nanometre-sized cavities and a high work function is an ideal candidate for supercapacitors with potential applications in handheld electronic devices, transportation, and renewable energy storage for power grids.

The discharging behaviour under a constant current of 1 pA, 1 nA, 1 μ A, and 1 mA after charging at DC currents of 1 mA for 30 s is shown in Fig. 1a,b for the APP and the dielectric polyvinylidene fluoride (PVDF, KF Piezo, Kureha) polymers, respectively. Increments in the charging current prolong the discharging time for both films. To evaluate the additionality (i.e., the integration effect) of their respective film capacitances, we investigated the constant-current discharging behaviour as a function of the surface area of both films. Fig. 1c,d show the 3 nA constant-discharging behaviour for the APP and PVDF polymers, respectively, after 1 mA–10 V charging. The former shows an increase in the discharging area (i.e., the storage energy) by increasing the surface area, whereas the behaviour of the latter is almost the same despite the increase film area. This means that each capacitor on the APP film is connected with a parallel circuit, i.e., with integrated capacitance. Strictly speaking, the surface structure of the APP film consists of an electric distributed

¹New Industry Creation Hatchery Centre, Tohoku University, Sendai, 980-8579, Japan. ²Waseda University Research Organization for Nano & Life Innovation, Green Device Laboratory, Tokyo, Japan. ³JEOL Ltd, Akishima, Tokyo 196-8558, Japan. Correspondence and requests for materials should be addressed to M.F. (email: fukuhara@niche.tohoku.ac.jp)

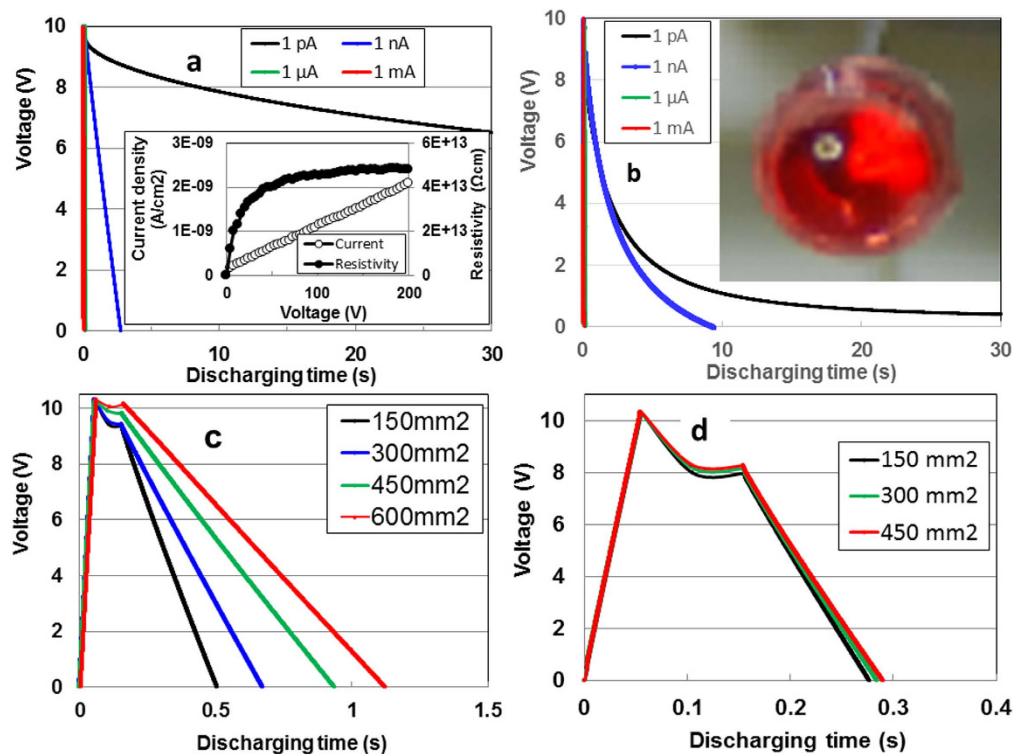


Figure 1. Discharging behaviour for the APP and PVDF devices after 1 mA–10 V charging. Constant-discharging (a,c) and integration effect on 3 nA-current discharging (b,d) for the APP and PVDF, respectively. Inset in (a): I - V and R - V characteristics, Inset in (b): illuminated LED light.

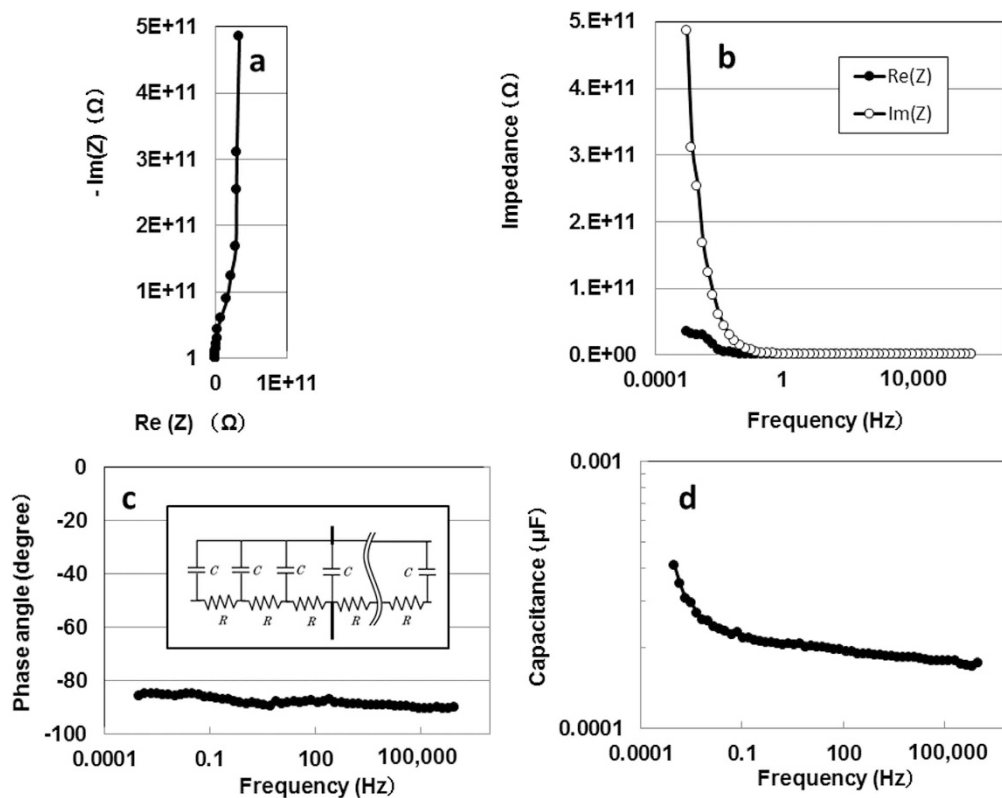


Figure 2. (a) Nyquist plot as a function of frequency for APP device. (b) Real and imaginary impedances. (c) Phase capacitance. (d) Series capacitance. Inset in (c): electric distributed constant-equivalent circuit of resistance and capacitance.

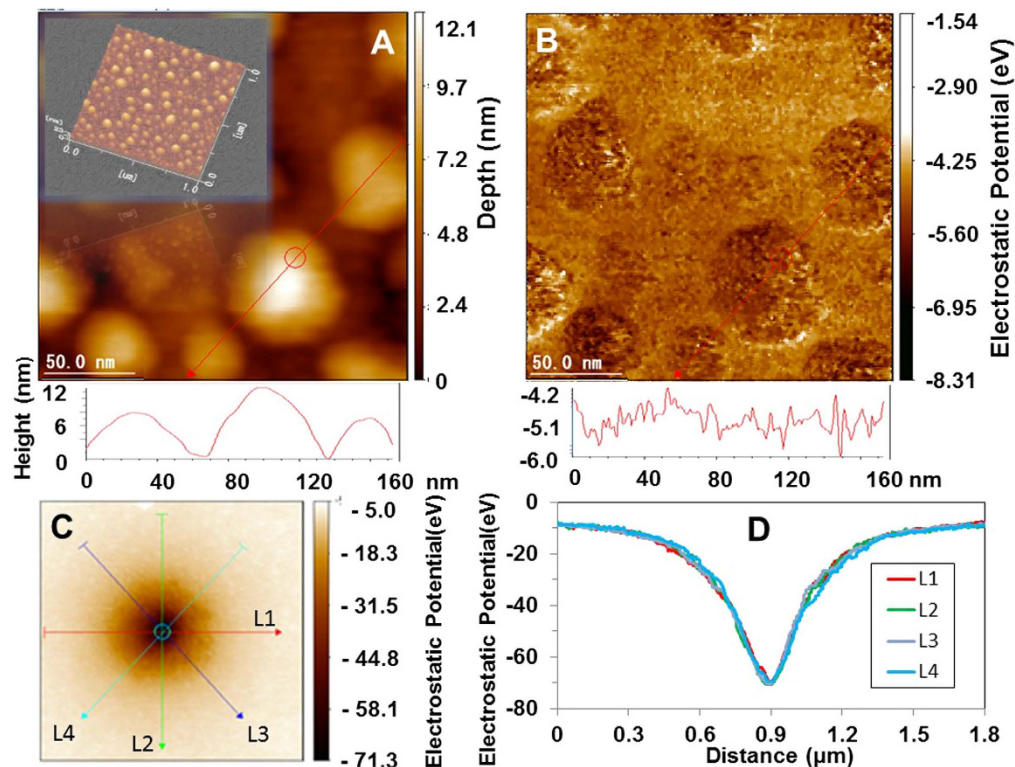


Figure 3. (a) AFM image of the APP surface. (b) Corresponding SKPM image. The lower profiles of (a,b) are the height from the valley bottom and the electrostatic potential for probe with 0 eV along red lines in upper images, respectively. (c) SKPM image. (d) Corresponding electrostatic profiles in four directions (L1, L2, L3 and L4) every 90° after applying an additional positive 20 V for 60 s at the centre of the Si back surface. Inset in (a): three-dimensional AFM image.

constant capacitor with low capacitance and high resistance ($\sim 48 \text{ T}\Omega\text{cm}$) (inset of Fig. 1a). Nevertheless, each capacitor on the PVDF film is connected by a series circuit, indicating the absence of an integration effect for electric storage. To provide visible evidence of the APP's electric storage, we illuminated a red LED light. The device, which has a surface area of 600 mm^2 , lit the LED for 3 ms (inset of Fig. 1b) after the device was charged with 1 mA at 10 V. The fact that we were able to light the LED confirms the potential for electric storage.

A complex plane plot of the impedance data obtained from the APP film is shown in Fig. 2a. The polymer's variation in impedance with frequency did not show the combined pattern of a line with a slope of 45°, which would associate it with the distributed resistance/capacitance in a porous electrode¹¹ and a high-frequency semicircle (i.e., a series-passive layer). A near-vertical line in the Nyquist plot suggests evidence of a series-RC circuit as well as a graphene double-layer capacitor¹². There were rapid increases in the imaginary impedance compared with the real impedance in the lower-frequency region (Fig. 2b). Moreover, the capacitive behaviour (near the -90° phase angle) all over the frequency region (Fig. 2c) is clear evidence of a series-RC circuit. Thus, APP films offer a near-ideal electric distributed constant structure (inset of Fig. 2c) for enhancing electric storage. However, the value of the series capacitance was 0.4 nF (178.8 nF/cm^3 , $88.9 \mu\text{F/kg}$) at 1 mHz (Fig. 2d).

We investigated the surface characteristics to understand the microscopic origin of the APP's higher electric storage. Figure 3a shows an atomic force microscope (AFM) image, and Fig. 3b shows the corresponding scanning Kelvin probe-force microscope (SKPM) image. These figures depict an uneven surface with a convexity of 28 nm in diameter and a concavity of 31 nm in length. The outside appearance of the surface bears a close resemblance to that of anodic oxidized amorphous TiO_{2-x} surfaces in previous papers^{8,9}. The line profiles of the noncontact AFM reveal spots that are distributed on the uneven surface. These spots have a high work function Φ , averaging 10.13 eV ($= 5.65 (\Phi_{Pt}) + 4.48 (\Phi_{CPD})$). This means that they can store electric charges; the same is true for the TiO_{2-x} layer⁸. The value of the work function is higher than 9.1 eV and was obtained from an ultraviolet photoelectron spectroscopy measurement¹³. After an additional positive 20 V was applied for 60 s at the centre of the Si back surface (see Fig. S5 in Supplementary Information), we observed an electrostatic potential distribution (Fig. 3c) and the corresponding electrostatic potential profiles in four directions (L1, L2, L3 and L4) every 90° (Fig. 3d). The potential negatively increased to -76.93 eV ($= 5.65 + 71.28 \text{ eV}$) at the centre. This value demonstrates the remarkable electric-absorption effect of the APP under applied voltage.

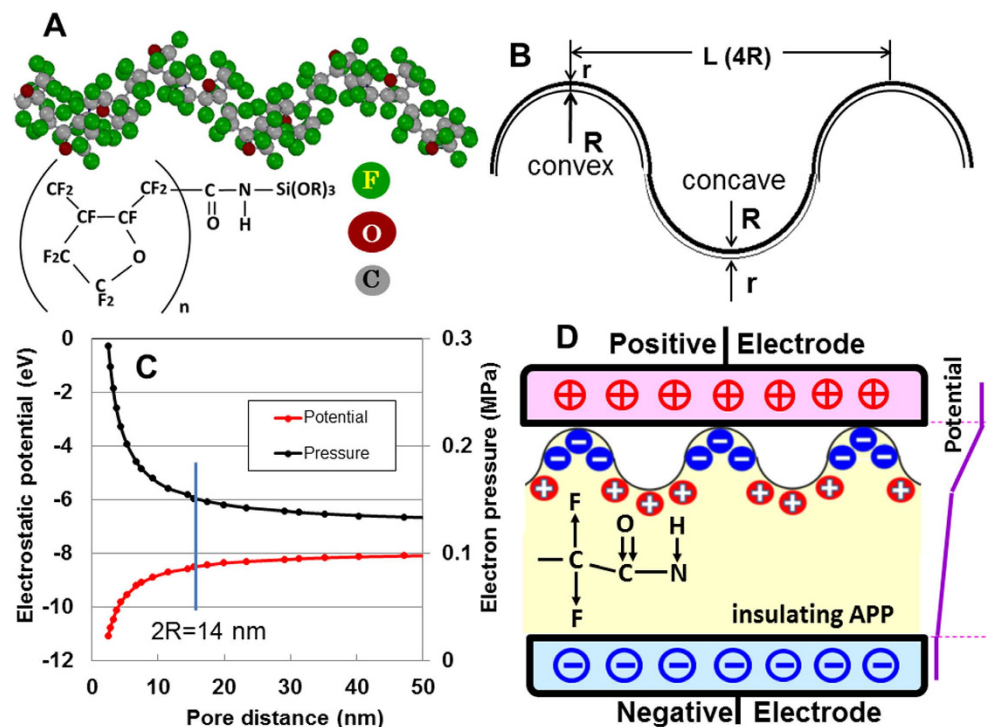


Figure 4. (a) Structural model of the APP with green fluorine, grey carbon, and red oxygen atoms, and possible structure with nanometer-sized clusters. (b) Schematic diagram for calculations based on the Thomas-Fermi statistical method. (c) Porous-distance dependence of the electron potential and pressure for the concave and convex portions. (d) Schematic representation of the microscopic electric energy storage used in this study.

We now turn to an explanation of the superior electric storage on the APP. The APP structure consists of PVDF main chains containing C=O and N-H radicles¹⁴ (Fig. 4a). The APP has rugged half-sphere surface (convex diameter of $2R$, Fig. 4b) with nanometre-sized cavities. Notably, lattice contractions have been observed in nanometre-sized metallic particles, such as silver¹⁵, copper and platinum¹⁶, and gold¹⁷. Such contractions are due to the extreme confinement of the inner electrons—the so-called quantum-size effect^{18,19}. This effect is interpreted by screening multiple inner-combined electrons for a strong positive-charge nucleus²⁰. Analogously, we inferred that the superior electric storage on the uneven APP surface is due to the same quantum-size effect, which induces a relative increase in the combined electrons, resulting in fewer free outer electrons from the screening effect. The convex-diameter dependencies of the calculated electrostatic potential and the induced outer electron pressure of fluorine atoms surrounding the APP structure are presented in Fig. 4c by means of the Thomas-Fermi (TF)'s electronic screening theory (discussed at length in the Supplementary Information). The decrease in diameter increases the negative potential and the positive pressure. The calculated potential was consistent with the experimental data at a convexity of 14 nm in diameter. A microscopic schematic is provided in Fig. 4d. In sharp contrast to conventional EDLC, in which its electrode is parallel to the circuit, the electrically- negative convex portion of APVEP main chains and the electrically-positive concave one dominated by C=O and N-H radicles with permanent dipoles²¹ form many electric double layers (EDLs) perpendicular to the electrode (see Fig. S4 in Supplementary Information). This model shows that the more an EDLs density increases (namely, the more convex-diameter decreases due to quantum-size effect), the more the electric storage increases. The uneven surface serves as a series of resistors for an insulation layer with tiny capacitors through the bulk, as shown in inset of Fig. 2c. Thus, in comparison with EDLCs, the APP device has some advantages, such as a wide operation temperature, higher charging/discharging voltage, larger integration, lighter weight, and prevention of IV drop at long distance from electrodes.

We demonstrated the storage potential for the APP given its nanometre-sized cavities on an uneven surface. The APP has a high work function, measured at 10.13 eV, and it succeeded in illuminating an LED. We inferred that the potential for electric storage is related to the quantum-size effect derived from the TF theory. The integration of the film with a micro-electro mechanical system is likely to provide even higher levels of charge storage for portable electric application.

Methods

The APVEP film with nanometre-cluster was prepared by doping a 3-aminopropyl (triethoxy) silane-coupling reagent into the APP. Sheet specimens with a thickness of $15\ \mu\text{m}$ were fabricated on the Si substrate by

spin-coating. The specific density, glass-transition temperature, and water-adsorption rate was 2.03, 471 K, and 0.01%, respectively²². The devices were fabricated mechanically⁸.

Scanning Kelvin probe-force microscopy (NC-AFM, JSPM-5200, JEOL) based on the measurement of electrostatic force gradient was applied to measure the absolute electrical potential between the Pt-coated cantilever tip at 0 and 20 V and the APP surface as the work-function difference. The DC charging/discharging behaviour was analysed at 10 V, 1 pA~1 mA for ~300 s at room temperature, with a complex impedance between 1 mHz and 1 M Hz and 10 mV, using the galvanostatic charge/discharge on a potentiostat/galvanostat (SP-150, BioLogic Science). A red LED lamp with standard power of 2×10^{-4} W was used to verify the electric storage.

References

1. Winter, M. & Brodd, R. J. What are batteries, fuel cells, and supercapacitors? *Chem. Rev.* **104**, 4245–4269 (2004).
2. Whittingham, M. Materials challenges facing electrical energy storage. *MRS Bull.* **33**, 411–419 (2008).
3. Conway, B. E. *Electrochemical Supercapacitors: Scientific Fundamentals and Technological Applications* (Plenum Press, New York, 1999).
4. Aricó, A. S., Bruce, P., Scrosati, B., Tarascon, J.-M. & Van Schalkwijk, W. Nanostructured materials for advanced energy conversion and storage devices. *Nat. Mat.* **4**, 366–377 (2005).
5. El-Kady, M. F., Strong, V., Dubin, S. & Kaner, R. B. Laser scribing of high-performance and flexible graphene-based electrochemical capacitors. *Science*. **335**, 1326 (2012).
6. Fukuhara, M., Araki, T., Nagayama, K. & Sakuraba, H. Electric storage in de-alloyed Si-Al alloy ribbons. *Europhys. Lett.* **99**, 47001 (2012).
7. Fukuhara, M. Electric charging/discharging characteristics of capacitor, using de-alloyed Si-20Al alloy ribbons. *Elect. Electro. Eng.* **3**, 72–76 (2013).
8. Fukuhara, M. *et al.* Superior electric storage in de-alloyed and anodic oxidized Ti-Ni-Si glassy alloy ribbons. *Phys. Stat. Sol. RRL*. **7**, 477–480 (2013).
9. Fukuhara, M. & Sugawara, K. Electric charging/discharging characteristics of super capacitor, using de-alloying and anodic oxidized Ti-Ni-Si amorphous alloy ribbons. *Nanoscale Res. Lett.* **9**, 253 (2014).
10. Yoshida, M. Contact electrification series of high polymer films. *Bull. Tomakomai Nat. Coll. of Tech.* **23**, 49–59 (1988).
11. Kötz, R. & Carlen, M. Principles and applications of electrochemical capacitors. *Electrochim. Acta.* **45**, 2483–2498 (2000).
12. Miller, J. R., Outlaw, R. A. & Holloway, B. C. Graphene double-layer capacitor with ac line-filtering performance. *Science*. **329**, 1637–1639 (2010).
13. Dao, T. T., Matsushima, T., Friedleine, R. & Murata, H. Controllable threshold voltage of a pentacene field-effect transistor based on a double-dielectric structure. *Org. Electronics*. **14**, 2007–2013 (2013).
14. Kashiwagi, T. *et al.* Nano-cluster-enhanced high-performance perfluoro-polymer electrets for energy harvesting. *J. Micromech. Microeng.* **21**, 125016 (2011).
15. Wasserman, H. J. & Vermaak, J. S. On the determination of a lattice contraction in very small silver particles. *Surf. Sci.* **22**, 164–172 (1970).
16. Wasserman, H. J. & Vermaak, J. S. On the determination of the surface stress of copper and platinum. *Surf. Sci.* **32**, 168–174 (1972).
17. Vermaak, J. S. & Kuhlmann-Wisdorf, D. Measurement of the average surface stress of gold as a function of temperature in the temperature range 50–985°. *J. Phys. Chem.* **72**, 4150–4154 (1968).
18. Paulus, P. M. *et al.* Surface and quantum-size effects in Pt and Au nanoparticles probed by ¹⁹⁷Au Mössbauer spectroscopy. *Phys. Rev. B*. **64**, 205418 (2001).
19. Aruna, I., Mehta, B. R., Malhotra, L. K. & Shivaprasad, S. M. Size dependence of core and valence binding energies in Pd nanoparticles: interplay of quantum confinement and coordination reduction. *J. Appl. Phys.* **104**, 064308 (2008).
20. Essén, H. Periodic table of the elements and the Thomas-Fermi atom. *Int. J. Quantum Chem.* **21**, 717–726 (1982).
21. Kumagai, T., Suga, T. & Kubono, A. High ordered structure of polyuria thin films prepared by vapor deposition polymerization. *Inst. Electri. Eng. Jpn. Trans. FM* **30**, 186–192 (2010).
22. Asahi Glass, Physical Characteristics of CYTOP, Production Information, List of Data (2015) (Data of access; 12/01/2016), <http://www.agc.com/kagaku/shinsei/cytop/physical.html>.

Acknowledgements

This work was supported by a Grant-in-Aid for Science Research (Grand Number AS2621258 L) in a Priority Area, “A-Step Program”, from the Japan Science and Technology (JST) Agency under the Ministry of Education, Culture, Sports Science, and Technology. The authors would like to thank K. Hatakeyama for help with molecular simulations, and K. Kashiwagi and Y. Kuwana from Asahi Glass Ltd. for helpful discussions.

Author Contributions

M.F. carried out the electric storage analysis and wrote the paper. F.H. edited the paper, and T.K. assisted with the electric measurements. T.S. carried out the structural analyses. All authors discussed the results and commented on the manuscript. M.F. supervised all of the work.

Additional Information

Supplementary information accompanies this paper at <http://www.nature.com/srep>

Competing financial interests: The authors declare no competing financial interests.

How to cite this article: Fukuhara, M. *et al.* Superior electric storage on an amorphous perfluorinated polymer surface. *Sci. Rep.* **6**, 22012; doi: 10.1038/srep22012 (2016).



This work is licensed under a Creative Commons Attribution 4.0 International License. The images or other third party material in this article are included in the article’s Creative Commons license, unless indicated otherwise in the credit line; if the material is not included under the Creative Commons license, users will need to obtain permission from the license holder to reproduce the material. To view a copy of this license, visit <http://creativecommons.org/licenses/by/4.0/>